Realtime bioelectrical data acquisition and processing from 128 channels utilizing the Wavelet-Transformation [1]

Andre Folkers [a] Florian Mösch [a] Thomas Malina [a]

Ulrich G. Hofmann [a]

[a] *Institute for Signal Processing, University of Lübeck, Germany*

Abstract

We propose a versatile signal processing and analysis framework for bioelectrical data, and in particular for neural recordings and EEG. Within this framework the signal is decomposed into subbands using fast wavelet transform algorithms, executed in real-time on a current DSP hardware platform. The decomposition is used to perform various processing and analysis tasks. Besides fast implementation of high, band, low pass filters, the decomposition is used for denoising and lossy, as well as lossless compression. Furthermore specific electrophysiologic analysis tasks like spike detection and sorting are performed within this decomposition scheme.

Key words: digital signal processor; data acquisiton; spike detection; wavelet transformation

1 Overview

Recording neural activity from a high number of neurons is a key issue in understanding how the brain works. Within the project VSAMUEL we developed successfully a versatile data acquisition system based on DSP boards [3]. The system is used for continous neural data acquisiton in vivo or in vitro with a high channel count (up to 128 channels) at sampling rate $F = 50$ kHz with a precision of 16 bits per sample. Important online data processing tasks include filtering and spike detection and classification, but also compression, transmission and storage. We propose a signal processing framework within which these tasks can be performed in an elegant way.

2 Wavelet transform and lifting scheme

The signal is decomposed into N+1 subbands by a N-level wavelet transform (WT). The subbands $d_j, j = 1, \ldots, N$ represent the frequency band $[F/2^{j+1}, F/2^{j+2}]$ and the subband a_N represents $[0, F/2^{N+1}]$. Fig. 1 shows the filter bank for $N = 3$. In each step the signal is decomposed by applying complementary filters to a_j, i.e. a high pass $\tilde{g}$ and a low pass $\tilde{h}$, which are determined by the selected wavelet. The results of both filter operations are subsampled by a factor of two, leading to subbands d_{j+1} and a_{j+1}. Note, that the number of coefficients in d_{j+1} and a_{j+1} is equal to the number of coeffi-

[1] This work has been supported by EU grant IST-1999-10073.

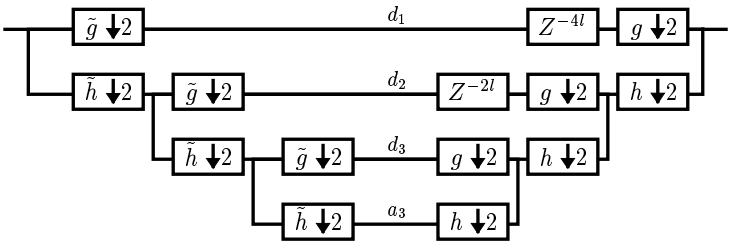

Fig. 1. Filter bank with three levels.

cients in a_j. The wavelet transform is implemented using the lifting scheme which is faster than the standard implementation (Fig. 1). It is done in-place, and with a small modification it implements a WT that maps integers onto integers [1] while preserving the possibility of perfect reconstruction. Therefore, this implementation of the WT is well suited for realtime processing using digital signal processors (DSP).

The lifting scheme provides another point of view to the wavelet transform. Basically it consists of three stages, which are a *split*, a *predict*, and an *update* stage as illustrated in Fig. 2 [6]. First the signal is split such that we obtain two sequences d_j and a_j which in our case consist of sample points with odd and with even indices, respectively. Now, we predict the values in d_j based on a_j as $P(a_j)$. Under the assumption that the signal is continous we have a good chance that our prediction is rather close to the actual values. We

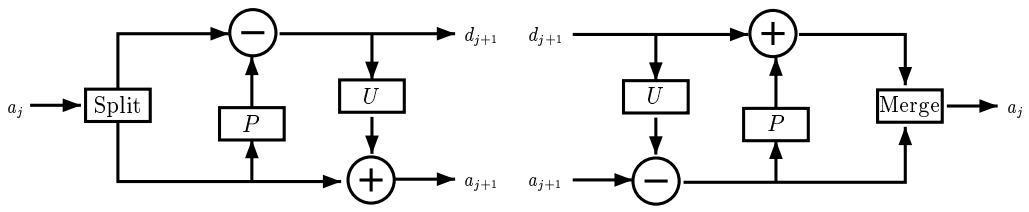

(a) Decomposition (b) Reconstruction

Fig. 2. Basic structure of the lifting scheme

compute the difference between prediction and actual values, and keep these values which are likely to be small: $d_{j+1} = d_{j+1} - P(a_{j+1})$. In order to preserve certain properties of the original signal in the coefficients a_j e.g. the mean value, we need the third stage, which is the update stage. Hereby, the values in a_j are modified by using an appropriate update operator on values in d_j and $U(d_j)$: $a_{j+1} = a_{j+1} + U(d_{j+1})$.

The perfect reconstruction property of the lifting scheme is obvious, because we can obtain a_j from a_{j+1} and d_{j+1} by inverting the data flow and the signs as shown in Fig. 2(b). Note, that this holds for arbitrary predict and update operators. Therefore, if these operators include a rounding to the next integer we obtain a wavelet transform that maps integer onto integers. It is possible to implement arbitrary wavelet transformations as shown in [1] by using multiple prediction and update operators sucessively. The respective operators are computed according to the given mother wavelet.

Using the lifting scheme and a routine optimized for our DSP, we can apply a six level Daubechies 2 decomposition filter bank on 32 channels sampled at 50 kHz in real time.

3 Filter

The decomposition allows a simple implementation of filters with different high pass, band pass, or low pass characteristics. Consider e.g. a neural recording

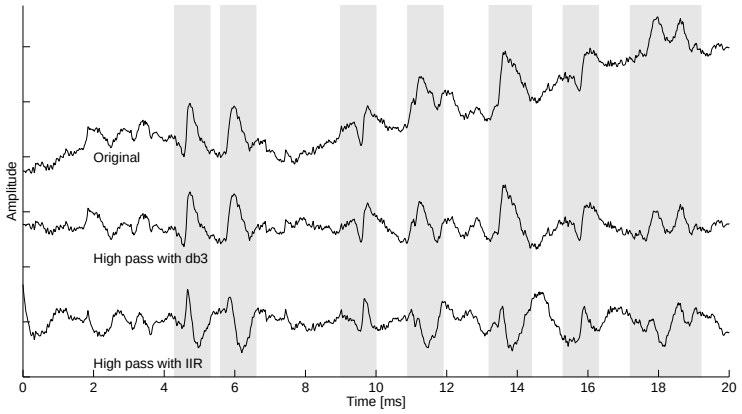

Fig. 3. High pass filtering using IIR versus elimination of wavelet approximation coefficients. The original neural recording has been decomposed with a 6 level WT using the Daubechies 4 wavelet. The coefficients of a_6 have been set to zero, corresponding to a high pass filtering with cut-off at 390.62 Hz. In a second approach the signal has been filtered by a 4-pole IIR high pass filter with cut-off at frequency 400 Hz, which was designed using the Butterworth method. Spike shapes in the IIR filtered result show significant distortions, while the spike shapes are apparently not distorted by the wavelet based high pass. Field potentials are eliminated well by both filters.

sampled at $F = 50$ kHz which contains both field potentials and action potentials. If it is decomposed by a 6-level WT into 7 subbands, then the field potentials are found in subband a_6. Setting the coefficients of a_6 to zero, eliminates the field potentials and corresponds to a high pass filter (Fig. 3). The respective low pass filter which eliminates the action potentials is obtained by setting the coefficients d_j for $j = 1, \ldots, 6$ to zero. A comparison of the results of both methods can be found in Fig. 3. Fig. 4 shows a comparison of the respective frequency responses. The decomposition also allows the implementation of band pass filters. Possible cut-off frequencies for band pass filter based on the WT are determined by the sampling rate and the number of levels. Arbitrary filters can be implemented if a Wavelet Packet Transform (WPT, see [8]) is utilized. However, the computation of the WPT transform

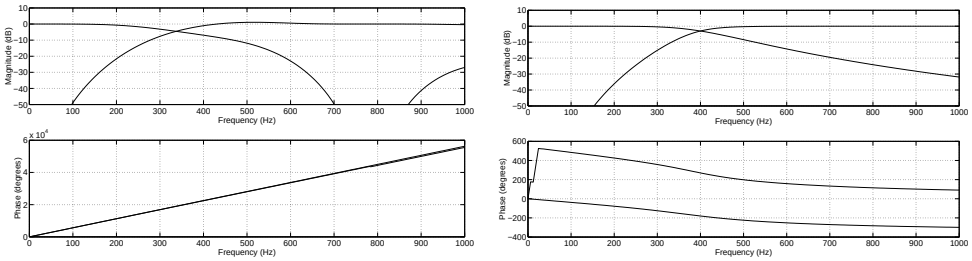

(a) Filter bank (b) IIR filter

Fig. 4. Comparison of filter bank based (a) and IIR (b) high and low pass filter. For the filter bank Daubechies wavelet with four vanishing moments has been used. The IIR filter have order 4 and cut off frequency at 400 Hz. The magnitudes of the frequency responses are comparable, but the phase of the filter bank is linear while the phase of the IIR filter is nonlinear, which is the reason for the distortions found in Fig. 3.

involves more operations than the WT. Because the number of operations has to be as low as possible to allow real-time computation on our DSP, we currently restrict ourselves to the WT.

4 Compression and Denoising

One important property of the WT is that it decorrelates the signal, i.e. the main information about the signal is collected in a few large coefficients, while the details are collected in many small coefficients. The average information content, also called *entropy*, can be computed as

$$E(s) = -\sum_{v \in \text{Values of } s} p(v) \log_2(p(v)), \tag{1}$$

where $p(v)$ is the probability of occurence of value v within signal s. The entropy is measured in bits per sample and since our signals are sampled in 16

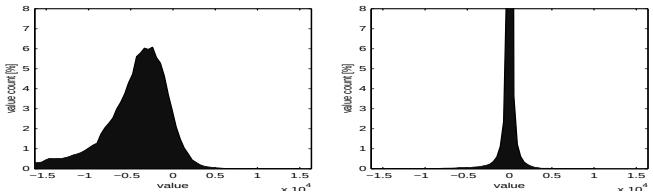

(a) Signal values (b) Wavelet coefficients

Fig. 5. Entropy reduction by wavelet transformation is illustrated by a comparison of the signal value and the wavelet coefficient histograms.

bit resolution, we can define the optimal achievable compression rate, e.g. with Huffman coding, as $E(s)/16$. The entropy of the decomposition is smaller than the entropy of the raw signal (Fig. 5). The entropy of a neural recording from a rat was quantified in [7] to be about 13.9 bits per sample and it is about 8.5 bits per coefficient for the decomposition. Therefore, the compression rate can be improved from 0.86 for the raw data down to 0.53 for the decomposition.

Another important task is the denoising of neural recordings. The typical background noise of neural recordings is mainly found in the first few levels $d_1, \ldots, d_3$ of the decomposition. Under the reasonable assumption that the background noise has a Gaussian distribution [5], a universal threshold can be found as $\delta = \sqrt{2\sigma^2 \log(n)}$ where σ^2 is the variance of the Gaussian noise and n is the length of the sequence [2]. Since the true variance σ^2 is usually unknown, it is estimated from the coefficients in d_1 which are dominated by the noise. We use the standard deviation estimator *median absolute deviation* (MAD): $\sigma^2 = \text{median}(|d_1|)/0.6745$. Using the median absolute value instead of the mean absolute value, this estimation is robust against large coefficients representing the signal that might occur in d_1.

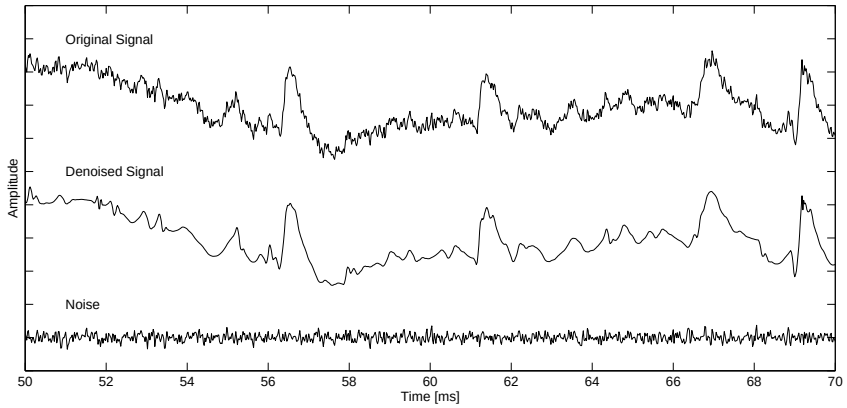

Fig. 6. Compression and Denoising. The comparison of the orginal neural signal at the top and the denoised signal in the middle reveals no apparent distortion of the signal. This is confirmed by the difference of signal and denoised signal, i.e. the removed noise, which is shown at the bottom. The entropy of the decomposition drops from 8.34 bits per sample down to 1.04 bits per coefficient. In other words the compression rate can be improved by a factor of 8.

Compression and denoising are closely related. The thresholded decomposition which represents the denoised signal has a much lower entropy than the original decomposition and thus can be compressed with a better rate. Depending on the chosen thresholds, the compression rate can reach values below 0.1 without losing a significant part of the signal. With the universal threshold for instance we obtain a compression rate of about 0.06 for neural recordings from a rat (Fig. 6). Lossy compression which does not distort the signal significantly is particularly usefull for longterm recordings.

5 Spike detection

The decomposition is used to analyse neural recordings. Spikes, for instance, are represented by a few large coefficients in subbands $d_2, \ldots, d_6$. Therfore, spike detection can be implemented by a threshold based method which uses

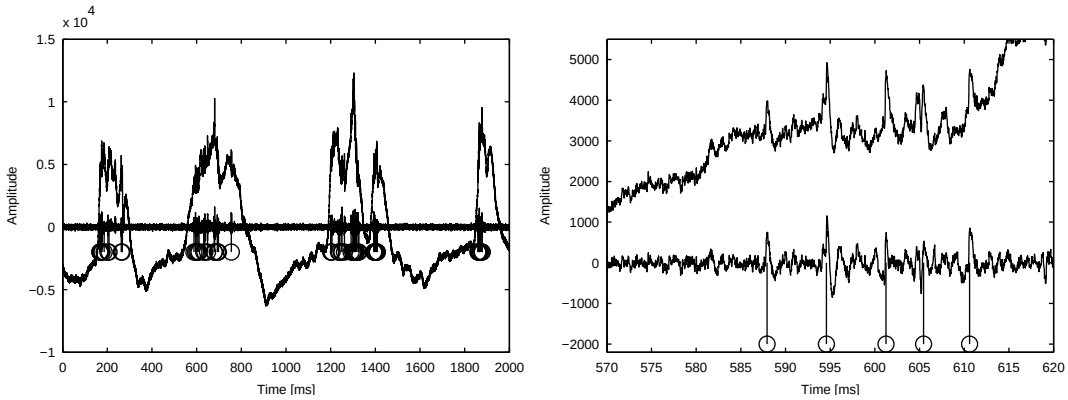

Fig. 7. Spike detection base on wavelet coefficients. Detected spikes are marked by stems. On the right an enlarged section of the signal is shown, which reveals that the signal to noise ratio is quite small, but still the spikes are detected well.

the wavelet coeffiecients. In Fig. 7 such a method has been used to detect spike in a neural recording from a rat, which contains field potentials and action potentials. In [4] another method to detect spikes based on wavelet coefficients is proposed.

6 Conclusions

Altogether we can state, that our DAQ system is able to record from a high number of channels, and furthermore it can perform sophisticated processing of the incoming electrophysiological data in realtime, which in our case is a wavelet decomposition. The data obtained from the wavelet decomposition represents the original data without loss, and it provides an elegant way to compress and to denoise the signals, and also to do further processing, like e.g. spike detection.

References

[1] I. Daubechies and W. Sweldens. Factoring wavelet transforms into lifting steps. *J. Fourier Anal. Appl.*, 4(3):245–267, 1998.

[2] David L. Donoho and Iain M. Johnstone. Ideal spatial adaptation by wavelet shrinkage. *Biometrika*, 81(3):425–455, 1994.

[3] A. Folkers and U.G. Hofmann. A multichannel data acquisition and analysis system based on off-the-shelf dsp boards. In *Proceedings of the EURASIP Conference on Digital Signal Processing for Multimedia Communications and Services*, Budapest, September 2001.

[4] H. Nakatani, T. Watanabe, and N. Hoshimiya. Detection of nerve action potentials under low signal-to-noise ratio condition. *IEEE Trans. on Biomedical Engineering*, 48(8):845–849, August 2001.

[5] Maneesh Sahani. *Latent Variable Models for Neural Data Analysis*. PhD thesis, California Institute of Technology, Pasadena, California, 1999.

[6] W. Sweldens. The lifting scheme: A new philosophy in biorthogonal wavelet constructions. In A. F. Laine and M. Unser, editors, *Wavelet Applications in Signal and Image Processing III*, pages 68–79. Proc. SPIE 2569, 1995.

[7] B. Weber, T. Malina, K. Menne, A. Folkers, V. Metzler, and U. G. Hofmann. Handling large files of multisite microelectrode recordings for the European VSAMUEL consortium. *Neurocomputing*, June 2001.

[8] Mladen Victor Wickerhauser. *Adapted Wavelet Analysis from Theory to Software*. A K Peters, Wellesley, Massachusetts, 1994.